CLINICAL ORAL IMPLANTS RESEARCH WILEY

A new device for improving dental implants anchorage: a histological and microcomputed tomography study in the rabbit

Journal:	*Clinical Oral Implants Research*
Manuscript ID:	COIR-Nov-14-OR-4452.R2
Manuscript Type:	Original Research
Date Submitted by the Author:	07-May-2015
Complete List of Authors:	Barak, Shlomo; Private Practice, Neuman, Moshe; Private Practice, Iezzi, Giovanna; University of Chieti-Pescara, Department of Medical, Oral and Biotechnological Sciences Piattelli, Adriano; University of Chieti-Pescara, Department of Medical, Oral and Biotechnological Sciences Perrotti, Vittoria; University of Chieti-Pescara, Dental School; Gabet, Yankel; Tel-Aviv University, Department of Anatomy & Anthropology
Keywords:	Animal Experiments, CT Imaging, Bone implant interactions

A new device for improving dental implants anchorage: a histological and microcomputed tomography study in the rabbit

Shlomo Barak, D.M.D., Private Practice, Tel Aviv, Israel*;

Moshe Neuman, D.M.D., M.Sc., Private Practice, Tel Aviv, Israel*;

Giovanna Iezzi, D.D.S., Ph.D., Researcher, Department of Medical, Oral and Biotechnological Sciences, University of Chieti-Pescara, Chieti, Italy*;

Adriano Piattelli, M.D., D.D.S., Professor of Oral Pathology and Medicine, Department of Medical, Oral and Biotechnological Sciences, University of Chieti-Pescara, Chieti, Italy;

Vittoria Perrotti, D.D.S., Ph.D., Post Doctoral Fellow, Department of Medical, Oral and Biotechnological Sciences, University of Chieti-Pescara, Chieti, Italy.

Yankel Gabet, D.M.D., Ph.D., Department of Anatomy & Anthropology, Sackler Faculty of Medicine, Tel Aviv University, Tel Aviv, Israel;

*These authors contributed equally to the study.

Running title: An electromagnetic cap improves implant anchorage.

Corresponding Author:

Dr. Vittoria Perrotti
Via dei Vestini,31
66100
Chieti (Italy)
Phone:+39-0871-3554083
Fax:+39-0871-3554076
E-mail: v.perrotti@unich.it

Abstract

Objective: In the present study, a new healing cap, that could generate a pulsed electromagnetic field (PEMF) around titanium implants to stimulate peri-implant osteogenesis, was tested in the rabbit model.

Materials and Methods: A total of 22 implants were inserted in the proximal tibial metaphysis of 22 rabbits. A healing cap containing the active device was inserted in half of the implants (11 test implants), an "empty" healing cap was inserted in the other ones (11 control implants). The animals were euthanized after 2 and 4 weeks, and the samples were processed for microcomputed tomography and histology. The peri-implant volume was divided into coronal (where the PEMF was the strongest) and apical regions.

Results: Most of the effects of the tested device were confined to the coronal region. Two weeks post-implantation, test implants showed a significant 56% higher trabecular bone fraction (BV/TV), associated with enhanced trabecular number (Tb.N, +37%) and connectivity density (Conn.D, +73%) as compared to the control group; at 4 weeks the PEMF induced a 69% increase in BV/TV and 34% increase of Tb.N. There was no difference in the trabecular thickness (Tb.Th) at either time point. Furthermore, we observed a 48% higher bone to implant contact (BIC) in the test implants versus controls after 2 weeks; this increase tended to remain stable until the fourth week. Mature trabecular and woven bone were observed in direct contact with the implant surface with no gaps or connective tissue at the bone-implant interface.

Conclusions: These results indicate that the PEMF device stimulated early bone formation around dental implants resulting in higher peri-implant BIC and bone mass already after 2 weeks which suggests an acceleration of the osseointegration process by more than 3 times.

Keywords: animal study, dental implants, healing cap, histology, microcomputed tomography, osseointegration.

Introduction

Titanium implants are widely used in dentistry due to their ability to form a tight connection with the surrounding bone. Despite new advancements and improvements of the commercially available implants, the conventionally recommended healing period during which implants should remain unloaded is 2 to 6 months. According to the latest reviews, shortening of this pre-loading time increases the failure rate by 2- to 3-fold, especially for unsplinted implants (Tawse-Smith et al. 2002; Esposito et al. 2009; Gallucci et al. 2009). Indeed, some prerequisites are necessary for an immediate loading of dental implants, such as primary clinical stability and adequate splinting. Quantity and quality of the bone tissue at the interface affect implant primary stability and therefore, the prognosis of immediately loaded implants (Degidi et al. 2009). Hence, the necessity of additional stimulants for enhanced osteogenesis in order to overcome the failures especially in poor quality bone and shorten the loading time.

After the experiments of Yasuda et al. (1955) on the effect of electrical stimulation on bone metabolism, electrically induced osteogenesis has been investigated both *in vivo* and *in vitro* (Yasuda et al. 1955; Spadaro 1997). Despite the clinical success, the underlying mechanism by which electrically induced osteogenesis occurs remains still unclear, and the operating principles of both static magnetic fields (SMF) and pulsed electromagnetic fields (PEMFs) on osteoblast differentiation and proliferation have been contradictory. However, it is known that biophysical inputs, including electric (EF) and electromagnetic fields (EMFs), regulate the expression of genes for structural extracellular matrix (ECM) proteins, resulting in acceleration in tissue repair. EF and EMFs can increase the synthesis of growth factors through activation of cell signal transductions, enhancing in this way endochondral bone formation (Aaron et al. 2004).

The electromagnetic field is a physical field produced by electrically charged objects. Magnetic fields surround and are created by electric currents, magnetic dipoles, and changing electric fields. Magnetic fields also have their own energy, with an energy density proportional to the square of the field intensity. The greater the current, the stronger the electromagnetic field. The electromagnetic field has 3-dimensional vectors with values defined at every point of space. Electromagnetic field treatment is a useful treatment modality that has been shown to be effective in a variety of medical conditions, especially in the healing of non-union bone fractures (Gupta et al. 2009; Goldstein et al. 2010), and this type of treatment tends to increase the mechanical strength of fractured bone (Bruce et al. 1987). A positive effect was reported in the improvement of the bone mineral density of osteoporotic women (Tabrah et al. 1990).

Bone growth can be stimulated by three different methods of EF/EMF: capacitive coupling using electrodes placed on the skin, direct current stimulation using implanted electrodes and electromagnetic stimulation by inductive coupling using time-varying magnetic fields. Clinical application of the latter category is possible through two different Food and Drug Administration (FDA)-approved technologies: PEMF and combined magnetic fields (Pilla, 2002). The use of PEMF was approved by the FDA in 1979 and has been used clinically for over 26 years thenceforth.

Magnetic fields and induced electrical fields influence cell response and gene expression (Bodamyali et al. 1998; Brighton et al. 2001). Pulsed electric magnetic fields (PEMFs) reduce cell number, increase osteoblast maturation, proliferation and differentiation, promote bone mineralization (Bodamyali et al. 1998; De Mattei et al. 1999; Brighton et al. 2001; Aaron et al. 2004), collagen synthesis, osteogenic differentiation (Wang et al. 2015) and production of local factors such as transforming growth factor–beta 1 (TGFβ1) (Lohmann et al. 2000). The application of PEMF induced osteogenic differentiation by increasing the manifestation of alkaline phosphatase (Chang et al. 2004), osteocalcin and matrix

mineralization (Ongaro et al. 2014). It is suggested that modulate the process of osteoclastogenesis and subsequent bone resorption (He et al. 2015).

PEMF effects in various clinical situations intended to increase bone regeneration. PEMF mainly influenced vascular growth and vascular formation (Greenough 1992) and neo-vascularization (Fu et al. 2014). Therefore enhanced the quality of re-vascularized tissue (Roland et al. 2000) and caused the expansion of fine arteries in mice muscles (Smith et al. 2004). PEMF treatment induced arteriolar dilation leading to an increase in microvascular blood flow and tissue oxygenation (Bragin et al. 2014).

In dental implants, the PEMF stimulation may be useful to promote bone formation around rough-surfaced dental implants (Matsumoto et al. 2000) and increase the amount of bone formation in order to achieve a shortened osseointegration period for the implants placed immediately after tooth extraction (Shayesteh et al. 2007). During bone healing removable prostheses are used; however, many patients find these temporary prostheses rather uncomfortable, and a shortening of the healing period without jeopardizing the implant success could have a great clinical value. Therefore, it was hypothesized that a new implant device, locally generating a PEMF, would significantly stimulate bone healing and increase bone density around implants, and hence make possible immediate and early loading.

The aim of the present study in the rabbit model was to evaluate, using microcomputed tomography (μCT) and histology, a new healing cap, that was temporarily connected with dental implants and that could generate a PEMF around them. This systems was developed based on positive results observed in other bone healing models, using conceptually similar systems that required an external power source and wiring, making this option inconvenient and inappropriate for dental implants (Matsumoto et al. 2000; Shayesteh et al. 2007; Leesungbok et al. 2011).

Materials and Methods

Study Design

The experimental protocol was designed according to ISO recommendations (International Standard ISO 10993-6, 1994) and approved by the Ministry of Health, Animal Care and Use Committee of the Ministry of Health, 2 Ben-Tabay St.-Jerusalem, Israel. Twenty two 4-month old male New-Zealand White rabbits were purchased from Harlan Laboratories (Rehovot, Israel) and maintained at the animal research facility of Hassaf Harofeh Medical Center, Tzrifin, Israel. Animals were fed purina (Koffolk 19-520, Koffolk Ltd., Tel Aviv, Israel) and water *ad libitum* throughout the experiment. After one week acclimation, a total of 22 commercially available dental implants (3.3 mm x 8 mm DFI implant, AlphaBio Tek, Petach Tikva, Israel) were inserted into the proximal metaphysis of one tibia in each animal. Half of the implants were sealed with an "empty" healing cap (control implants) while in the other half of the implants (test implants) a healing cap containing the PEMF-emitting ('active') device was placed (Fig. 1). One animal did not survive the anesthesia and implantation procedure, and one animal was euthanized due to weigh loss of more than 10%; four additional animals were excluded due to either non-standard implant positioning, swelling or scarification at the implantation site. Animals were killed after 2 and 4 weeks; a total of 16 samples were processed for μCT analysis (n=4 for each time/treatment group), and 4 for the histology.

Surgical Procedure

All surgical procedures were carried out under general anesthesia using a mixture of 35 mg/kg of ketamine hydrochloride (Amgen Technology, Dublin, Ireland). Before implant surgery, 0.5 mL of a mixture of Lidocain hydrochloride (2%) and adrenaline (1:100000) (Teva, Petach Tikva, Israel) was subcutaneously injected at the knee for local anesthesia. Anesthesia efficiency was checked by the absence of pupillary and corneal reflexes, and vitals were monitored throughout the surgery. Starting on the day of surgery, animals were administered Dipyrone (Optalgin, 5 mg/Kg, twice a day) (Teva,

Budapest, Hungary), and a cefalosporin antibiotic (Ceftrioxan, 30 mg/Kg/day, twice a day) (Paramus, NY, USA) for one week.

Under sterile conditions and using saline cooling and low-speed hand-piece, an insertion path was prepared in the proximal tibial metaphysis perpendicular to the cortex towards the postero-lateral ridge using a round low speed dental bur, 1.5 mm in diameter. The cortical penetration hole was prepared 1.5 mm distal to the proximal growth plate, which was visible as a line brighter than the bone. Accuracy was ensured by using live x-ray fluoroscopy. The path extended through the cortex and trabecular bone, with the opposite cortex left imperforated. A pilot drill of 2 mm was used and a final drill of 2.8 mm diameter was performed before threading the implant shaft. Half of the implants were threaded with an "empty" healing cap, while the other half were threaded with an activated electromagnetic healing cap that consisted of a battery, an electronic device and an induction coil. The procedure was completed by repositioning the soft tissues and suturing the skin incision to completely cover the implant and healing cap using internal and external resorbable Vicryl 4-0 sutures (Ethicon, West Somerville, NY, USA). The animals wore an Elizabethan collar to avoid self-injury at the implant site.

Intensity of the magnetic field was monitored during the *in vivo* experiments, before implant insertion in the rabbits, and again before euthanasia. Notably, no decrease of the intensity was observed after either 2 or 4 weeks of continuous operation. At the end of the experimental period, the animals were euthanized using an intravenous administration of Ketamin HCl at 2 and 4 weeks after surgery, and bone specimens including the implants were collected.

Micro-Computed Tomography

At the time of euthanasia, tibiae with implants were separated, transferred for 48 h to phosphate buffered formalin and then kept in 70% ethanol. The proximal 20 mm of the tibiae including the implant were then scanned using a 3D x-ray microscopy system XCT400 (Xradia, Pleasanton, CA, USA). For image acquisition, the specimens were mounted and tightly fixed to the sample holder, so

that the long axis of the implant was perpendicular to the x-ray beams. The X-ray tube voltage was set to 80 kV, in order to allow maximal X-ray transmission through the highly opaque titanium implant. To maximize signal-to-noise ratio, the system was operated at 100 µA and 300 msec integration time for a total of 2000 projections. CT images were reconstructed and stored in 3-D arrays with an isotropic voxel size of 19 µm. A constrained 3-D Gaussian filter (sigma=1.2 and support=1) was used to partly suppress the noise in the volumes.

Three-dimensional morphometric analysis

To test the bone response to the electric field generated by the device housed in the healing cap, structural parameters of the trabecular peri-implant bone were analyzed using a global 3D approach. Due to the steep gradient in trabecular bone fraction as the distance from the primary spongiosa increases (Gabet et al. 2008), the region of interest was predefined anatomically relative to the tibial proximal growth plate. This volume was delineated proximally by a cross-sectional plane located 0.6 mm from the most distal fold of the primary spongiosa and extended 4.5 mm distally. In the radial dimension, the peri-implant region included the trabecular bone up to a distance of 1 mm from the implant surface. The analyses were performed separately into two subregions, where the region from the healing abutment to half the length of the implant was defined as “coronal” region, and the other half as the “apical” region (Fig. 2). The cortical bone and the part of the implant shank in contact with cortical bone were excluded from the analysis. The titanium and mineralized tissue were separated from each other and from the bone marrow, including the immediate implant vicinity, by applying a multi-level thresholding procedure (Muller & Ruegsegger 1997; Gabet et al. 2006). The %OI (a.k.a. bone-to-implant contact, BIC) was calculated as the ratio between bone and total voxels in contact with the implant (Gabet et al. 2006; Gabet et al. 2008). The following morphometric parameters were also calculated in the peri-implant trabecular bone (PIB): trabecular bone volume fraction (BV/TV),

trabecular thickness (Tb.Th), trabecular number (Tb.N), trabecular spacing (Tb.Th) and connectivity density (Conn.D).

Statistical analysis

Values are represented as Mean ± SD. Analysis was performed by two-way-ANOVA with treatment type (PEMF or control cap) and time after implant insertion as independent factors. Holm Sidak's post-test was used to compare treatments. Statistically significant difference was defined as $p<0.05$. All the calculations were performed using GraphPad (San Diego, CA, USA) Prism version 6.01.

Histological analysis

Four representative specimens (one per group) were processed to obtain thin histologic slides of the bone and implant. The specimens were dehydrated in a graded series of ethanol rinses and embedded in a glycolmethacrylate resin (Technovit 7200 VLC, Kulzer, Wertheim, Germany). After polymerization, the specimens were sectioned, along their longitudinal axis, with a high precision diamond disk at about 150 µm and ground down to about 30 µm with a specially designed grinding machine Precise 1 Automated System (Assing, Rome, Italy). Three slides were obtained from each specimen. These slides were stained with acid fuchsine and toluidine blue and examined with transmitted light Leitz Laborlux microscope (Leitz, Wetzlar, Germany). Histomorphometry of the percentages of bone-to-implant contact (BIC) was carried out using a light microscope (Laborlux S, Leitz, Wetzlar, Germany) connected to a high-resolution video camera (3CCD, JVC KY-F55B, JVC®, Yokohama, Japan) and interfaced to a monitor and PC (Intel Pentium III 1200 MMX, Intel®, Santa Clara, CA, USA). This optical system was associated with a digitizing pad (Matrix Vision GmbH, Oppenweiler, Germany) and a histomorphometry software package with image capturing capabilities (Image-Pro Plus 4.5, Media Cybernetics Inc., Rockville, MD, USA,).

Results

Electromagnetic field generated by tested device

The tested device generated an electro-magnetic field at frequency of 10 Hz and intensity of 0.4 to 0.2 mTesla at distances of 1 and 2 mm away from the implant surface, respectively, with a steep gradient, both longitudinally (along implant long axis) and radially.

Three-dimensional structural analysis

There were no noticeable signs of infection or inflammation in any of the animals included in this study. In all included specimens the long axis of implant was located 2.1±0.483 mm from the distal-most invagination of the growth plate. Because the electromagnetic field generated by the device decreased as the distance from the engineered healing cap increased, bone response was calculated separately in the "coronal" and the "apical" peri-implant regions. All the μCT data statistical analyses are presented in Table 1 and Figs. 2-4. Overall, during the 4-week follow-up period, the %OI was significantly increased by the PEMF cap (p=0.0102). In the test group, the %OI was 49% and 42% higher than in the control group at the 2 and 4-week time points. Around the entire length of the implant (full region) %OI was stimulated by 23% on average over the entire follow-up period (p=0.0283, Fig. 4). In the apical region however, %OI was not significantly affected by the PEMF cap (Fig. 4). Interestingly, the osteogenic effect of the PEMF cap was not restricted to the bone-implant contact but also significantly affected the peri-implant trabecular bone. Two and four weeks post-implantation, morphometric analysis in the coronal area revealed a 56% and 69% increase in the trabecular BV/TV as compared to the control group (p= 0.045 and p=0.019, respectively, Fig. 3). This clearly indicates that the strong anabolic effect induced by the active cap during the first 2 weeks was maintained even after 4 weeks. During the 4-week post-implantation period, the increased BV/TV related to the active caps was associated with significantly higher Tb.N and Conn.D in the coronal

region (p=0.009 and p=0.0164, respectively). Already after 2 weeks, Tb.N and Conn.D were increased by 37 and 73%, respectively. Of note, the magnetic field targeted specifically the formation of new trabeculae, as indicated by the stimulation of %OI, Tb.N and Conn.D. This conclusion was further supported by the fact that the thickness of existing trabeculae (Tb.Th) remained unaffected. In line with the increased Tb.N, the trabecular spacing was reduced by ~29% at both the 2 and 4-week time points (p=0.0204).

As expected from the reduced magnetic intensity at the distant end of the implant, we found no effect on %OI and any of the morphometric trabecular bone parameters in the apical subregion. In both the control and test groups, the peri-implant BV/TV significantly decreased between 2 and 4 weeks post-surgery, in the combined apical and coronal regions (full region, p=0.0138) due a significant decrease in the apical subregion only (p=0.0173). In the coronal region, the temporal decrease was not significant (Fig. 4). Together our results showed that the PEMF device significantly stimulated osteogenesis over the entire 4-week follow-up period. Moreover, the peak effect was generally reached already at the 2-week time point.

Histological analysis

In the control group between 2 and 4 weeks post-surgery, the BIC was 54.2% and 70%, respectively. Two weeks post-surgery, in the coronal portion, it was possible to observe the presence of newly formed bone between the pre-existing cortical bone and the implant surface (Fig. 5). In the apical portion, many newly formed bone trabeculae could be observed in the vicinity of the implant. Four weeks post-surgery, trabecular mature bone was present around the coronal portion of the implant. Bone trabeculae were found directly on the implant surface in the coronal and apical portions of the implant.

In the test group between 2 and 4 weeks post-surgery, the BIC was 74.3%.and 85.3%, respectively. Two weeks post-surgery, the trabecular peri-implant bone with many marrow spaces was present; bone trabeculae were found directly on the implant surface in the coronal, middle and apical portions of the implant (Fig. 5). Four weeks post-surgery, lamellar and woven bone types were observed in direct contact with the implant surface; no gaps or connective tissue were present at the bone-implant interface. Bone trabeculae were present in the apical portion of the implant (Fig. 5).

Discussion

A faster and more effective fixing of titanium implants into bone, reducing patient morbidity and improving the success rate of such implants in reconstructive dental and orthopedic treatments, is still an enduring challenge nowadays. A rapid and successful osseointegration has a pivotal role in implant fixation and the desire to accelerate and improve osseointegration leads many implantology investigations and development efforts. Biophysical stimulation represents a non-invasive and locally applied strategy to enhance bone regeneration around implants.

Electromagnetic stimulation is known to promote osteogenesis activity and several studies have shown its clinical effect using electromagnetic field from external source (Ozen et al. 2004). In dentistry, there were studies that examined the impact of electromagnetic stimulation on bone formation and growth (Matsumoto et al. 2000). These studies have shown a decrease in duration of osseointegration around dental implants using external source of electromagnetic field. In this study, it is the first time that the source of the electromagnetic field is directed internally to the dental implant by using an active healing cap device. This device was able to produce the same electromagnetic field around the implant as external devices. The advantage of this device was that the effective electromagnetic field was only around the dental implant and that there was no need to use an external source. This fact allowed

activating the electromagnetic field continually for 24 hours a day, thus achieving better results compared to an interrupted treatment by an external device. Moreover, patient compliance would not interfere with the treatment. The present study showed that PEMF could induce osseointegration around dental implants in the rabbit tibia. The possible mechanism of PEMF on osteogenesis included induction of vascularization, osteogenic cell proliferation, activation, and collagen production (Ongaro et al. 2014). Our results could be explained by a recent study finding that PEMF increased the number of osteoblasts attached to the implant surface, increased the number of microfilaments and pseudopodia formed by the osteoblasts, the increased cell proliferation on the implant surface and the stimulated extracellular matrix mineralization (Korenstein et al. 1984; Goodman et al. 1985; Wang et al. 2014). Moreover, PEMF appears to affect already differentiated bone cells through various transduction pathways and growth factors, decreasing osteoclastic resorption and increasing osteoblastic bone formation (Taylor et al., 2006).

Several studies showed that devices providing an external source of PEMF resulted in a significantly greater bone to implant contact and bone density around the implant (Shimizu et al. 1988; Matsumoto et al. 2000; Fini et al. 2002; Fini et al. 2006). In the present study, the healing cap attached to the implant to generate a localized PEMF was able to produce a similar effect, i.e. increased bone to implant contact and bone density around the implant. The duration of stimulation was an important factor. A study by Buzzà et al. (2003) assessed that PEMF stimulation does not improve the bone-healing process around implant in tibiae metaphysis of white rabbits. However, PEMF was applied only 30 minutes per day. In a study by Grana et al. (2008) thirty rats were treated with PEMF (72 mT 50Hz), twice a day in sessions of 30 minutes each and short daily electromagnetic stimulation appeared to be a promising treatment for acceleration of both bone-healing and peri-implant bone formation. Furthermore, it has been shown that stimulation of 10 h/day promotes better bone formation around dental implant compared to stimulation of 5h/day (Matsunaga 1986; Ijiri et. al. 1996). Hence,

applying a PEMF stimulation for a more extended lapse of time may lead to achieve better results. The healing cap used in the present study generated an electro-magnetic field, 24h/day every day, with a steep gradient. Magnetic field intensity was the greatest in the analyzed coronal region as compared with the apical region and at a distance of 1 mm from the implant surface. The tested device stimulated early bone formation around the coronal part of implants leading to increased % OI and BV/TV after 2 weeks, and this bone stimulating effect lasted for at least 4 weeks in vivo. The magnetic field generated by the device targeted primarily the peri-implant bone in the coronal half of the implant length, a region that was particularly sensitive to bone resorption because of the concentration of mechanical stresses during occlusal loading. Interestingly, the increase in PIB density was due to an increase in the number of bone trabeculae, while the average thickness of the trabeculae remained unaffected. This observation indicates that the electromagnetic field did not affect bone turnover in the preexisting trabeculae but rather stimulates *de novo* bone formation.

Previous reports show that the peak of %OI and BV/TV around titanium implants in rabbits is generally reached after more than 6 weeks (Munhoz et al. 2012). Together with our data demonstrating that the peak is reached already after 2 weeks, it is implied that the electromagnetic healing cap accelerates implant osseointegration by more than 3 times. Moreover, in a similar model in rats, highly significant correlations between changes in % OI and BV/TV on one hand and the biomechanical properties on the other hand were found (Gabet 2006; Gabet 2010). It is reasonable to assume that the herein reported structural effect of the magnetic field will also improve the implant mechanical anchorage.

Based on these results showing accelerated bone formation on and around dental implants, it could be suggested that the latent time for osseointegration in dental implants can be reduced by 3-times and the success rate in implants in poor quality bone could be increase by using an electromagnetic healing cap.

References

Aaron, R.K., Boyan, B.D., Ciombor, D.M., Schwartz, Z. & Simon, B.J. (2004) Stimulation of growth factor synthesis by electric and electromagnetic fields. *Clinical Orthopaedic and Related Research* **419**:30-37.

Bodamyali, T., Bhatt, B., Hughes, F.J., Winrow, V.R., Kanczler, J.M., Simon, B., Abbott, J., Blake, D.R. & Stevens, C.R. (1998) Pulsed electromagnetic fields simultaneously induce osteogenesis and upregulate transcription of bone morphogenetic proteins 2 and 4 in rat osteoblasts in vitro. *Biochemical and Biophysical Research Communication* **250**:458-461.

Bragin, D. E., Statom, G. L., Hagberg, S. & Nemoto, E. M. (2014) Increases in microvascular perfusion and tissue oxygenation via pulsed electromagnetic fields in the healthy rat brain. *Journal of Neurosurgery*: 1-9.

Brighton, C.T., Wang, W., Seldes, R., Zhang, G. & Pollack, S.R. (2001) Signal transduction in electrically stimulated bone cells. *Journal of Bone and Joint Surgery. American volume* **83-A**:1514-1523.

Bruce, G.K., Howlett, C.R. & Huckstep, R.L. (1987) Effect of a static magnetic field on fracture healing in a rabbit radius. Preliminary results. *Clinical Orthopaedic and Related Research* **222**:300-306.

Buzzá, E.P., Shibli, J.A., Barbeiro, R.H. & Barbosa, J.R. (2003) Effects of electromagnetic field on bone healing around commercially pure titanium surface: histologic and mechanical study in rabbits. *Implant Dentistry* **12**:182-7.

Chang, W. H., Chen, L. T., Sun, J. S. & Lin, F. H. (2004) Effect of pulse-burst electromagnetic field stimulation on osteoblast cell activities. *Bioelectromagnetics* **25**: 457-465.

Degidi, M., Iezzi, G., Perrotti, V. & Piattelli, A. (2009) Comparative analysis of immediate functional loading and immediate nonfunctional loading to traditional healing periods: a 5-year follow-up of 550 dental implants. *Clinical Implant Dentistry and Related Research* **11**: 257-266.

De Mattei, M., Caruso, A., Traina, G.C., Pezzetti, F., Baroni, T. & Sollazzo, V. (1999) Correlation between pulsed electromagnetic fields exposure time and cell proliferation increase in human osteosarcoma cell lines and human normal osteoblast cells in vitro. *Bioelectromagnetics* **20**:177-182.

Esposito, M., Grusovin. M.G., Achille, H., Coulthard, P. & Worthington, H.V. (2009) Interventions for replacing missing teeth: different times for loading dental implants. *Cochrane Database of Systematic Reviews*: CD003878

Fini, M., Cadossi, R., Cane, V., Cavani, F., Giavaresi, G., Krajewski, A., Martini, L., Aldini, N. N., Ravaglioli, A., Rimondini, L., Torricelli, P. & Giardino, R. (2002) The effect of pulsed electromagnetic fields on the osteointegration of hydroxyapatite implants in cancellous bone: A morphologic and microstructural in vivo study. *Journal of orthopaedic research* **20**: 756-763.

Fini, M., Giavaresi, G., Giardino, R., Cavani, F. & Cadossi, R. (2006) Histomorphometric and mechanical analysis of the hydroxyapatite-bone interface after electromagnetic stimulation: An experimental study in rabbits. *The Journal of bone and joint surgery. British volume* **88**: 123-128.

Fu, Y. C., Lin, C. C., Chang, J. K., Chen, C. H., Tai, I. C., Wang, G. J. & Ho, M. L. (2014) A novel single pulsed electromagnetic field stimulates osteogenesis of bone marrow mesenchymal stem cells and bone repair. *PloS one* **9**: e91581.

Gabet, Y., Muller, R., Levy, J., Dimarchi, R., Chorev, M., Bab, I. & Kohavi, D. (2006) Parathyroid hormone 1-34 enhances titanium implant anchorage in low-density trabecular bone: a correlative micro-computed tomographic and biomechanical analysis. *Bone* **39**: 276-282.

Gabet, Y., Kohavi, D., Kohler, T., Baras, M., Muller, R. & Bab, I. (2008) Trabecular bone gradient in rat long bone metaphyses: mathematical modeling and application to morphometric measurements and correction of implant positioning. *Journal of Bone and Mineral Research* **23**:48-57.

Gabet, Y., Kohavi, D., Voide, R., Mueller, T. L., Muller, R. & Bab, I. (2010) Endosseous implant anchorage is critically dependent on mechanostructural determinants of peri-implant bone trabeculae. *Journal of Bone and Mineral Research* **25**: 575-583.

Gallucci, G.O., Morton, D. & Weber HP. (2009) Loading protocols for dental implants in edentulous patients. *International Journal of Oral & Maxillofacial Implants* **24**:132-146.

Goldstein, C., Sprague, S. & Petrisor, B. (2010) Electrical stimulation for fracture healing: current evidence. *Journal of Orthopaedic Trauma* **24**:S6.

Greenough, C. G. (1992) The effects of pulsed electromagnetic fields on blood vessel growth in the rabbit ear chamber. *Journal of Orthopaedic Research* **10**: 256-262.

Goodman, R., Abbot, J., Krim, A. & Henderson, A. (1985) Nucleic acid and protein synthesis in cultured Chinese hamster ovary (CHO) cells exposed to the pulsed electromagnetic fields. *Journal of Bioelectromagnetics* **4**: 565–576.

Grana, D.R., Marcos, H.J. & Kokubu, G.A. (2008) Pulsed electromagnetic fields as adjuvant therapy in bone healing and peri-implant bone formation: an experimental study in rats. *Acta Odontológica Latinoamericana* **21**:77-83.

Gupta, A.K., Srivastava, K.P. & Avasthi, S. (2009) Pulsed electromagnetic stimulation in ion of tibial diaphyseal fractures. *Indian Journal of Orthopaedic* **43**:156-160.

He, J., Zhang, Y., Chen, J., Zheng, S., Huang, H. & Dong, X. (2015) Effects of pulsed electromagnetic fields on the expression of nfatc1 and caii in mouse osteoclast-like cells. *Aging Clinical and Experimental Research* **27**: 13-19.

Ijiri, K., Matsunaga, S., Fukuyama ,K., Maeda. S., Sakou. T., Kitano. M. & Senba, I. (1996) The effect of pulsing electromagnetic field on bone ingrowth into a porous coated implant. *Anticancer Research* **16**:2853-2856.

Korenstein, R., Somjen, D., Fischler, H. & Binderman, I. (1984) Capacitative pulsed electric stimulation of bone cells. Induction of cyclic-AMP changes and DNA synthesis. *Biochimica et Biophysica Acta* **803**:302-7.

Leesungbok, R., Ahn, S.J., Lee, S.W., Park, G.H., Kang, J.S. & Choi, J.J. (2011) The effects of a static magnetic field on bone formation around a SLA treated titanium implant. *Journal of Oral Implantology* **39**:248-255.

Lohmann, C.H., Schwartz, Z., Liu, Y., Guerkov, H., Dean, D.D., Simon, B. & Boyan, B.D. (2000) Pulsed electromagnetic field stimulation of MG63 osteoblast-like cells affects differentiation and local factor production. *Journal of Orthopaedic Research* **18**:637-646.

Matsumoto, H., Ochi, M., Abiko, Y., Hirose, Y., Kaku, T. & Sakaguchi, K. (2000) Pulsed electromagnetic fields promote bone formation around dental implants inserted into the femur of rabbits. *Clinical Oral Implants Research* **11**:354-360.

Matsunaga S. (1986) Histological and histochemical investigations of constant direct current stimulated intramedullary callus. *Nihon Seikeigeka Gakkai Zasshi.* **60**:1293-1303.

Muller, R., Ruegsegger P. (1997) Micro-tomographic imaging for the nondestructive evaluation of trabecular bone architecture. *Studies in Health Technology and Informatics* **40**:61-79.

Munhoz, E. A., Bodanezi, A., Cestari, T. M., Taga, R., de Carvalho, P. S. & Ferreira, O., Jr. (2012) Long-term rabbits bone response to titanium implants in the presence of inorganic bovine-derived graft. *Journal of Biomaterials Applications* **27**: 91-98.

Ongaro, A., Pellati, A., Bagheri, L., Fortini, C., Setti, S. & De Mattei, M. (2014) Pulsed electromagnetic fields stimulate osteogenic differentiation in human bone marrow and adipose tissue derived mesenchymal stem cells. *Bioelectromagnetics* **35**: 426-436.

Ozen, J., Atay, A., Oruc, S., Salkiz, M., Beydemir, B. & Develi, S. (2004) Evaluation of pulsed electromagnetic fields on bone healing after implant placement in the rabbit mandibular model. *Turkish Journal of Medical Sciences* **35**:91-95.

Pilla, A.A. (2002) Low-intensity electromagnetic and mechanical modulation of bone growth and repair: are they equivalent? *Journal of Orthopaedic Science* **7**:420-428.

Roland, D., Ferder, M., Kothuru, R., Faierman, T. & Strauch, B. (2000) Effects of pulsed magnetic energy on a microsurgically transferred vessel. *Plastic and Reconstructive Surgery* **105**: 1371-1374.

Shayesteh, Y.S., Eslami, B., Dehghan, M.M., Vaziri, H., Alikhassi, M., Mangoli, A & Khojasteh, A. (2007) The effect of a constant electrical field on osseointegration after immediate implantation in dog mandibles: a preliminary study. *Journal of Prosthodontics* **16**:337-342.

Shimizu, T., Zerwekh, J. E., Videman, T., Gill, K., Mooney, V., Holmes, R. E. & Hagler, H. K. (1988) Bone ingrowth into porous calcium phosphate ceramics: Influence of pulsing electromagnetic field. *Journal of orthopaedic research* **6**: 248-258.

Smith, T. L., Wong-Gibbons, D. & Maultsby, J. (2004) Microcirculatory effects of pulsed electromagnetic fields. *Journal of orthopaedic research* **22**: 80-84.

Spadaro, J.A. (1977) Electrically stimulated bone growth in animals and man. Review of the literature. *Clinical Orthopaedics and Related Research* **122**:325-332.

Tabrah, F., Hoffmeier, M., Gilbert, F. Jr, Batkin, S. & Bassett, C.A. (1990) Bone density changes in osteoporosis-prone women exposed to pulsed electromagnetic fields (PEMFs). *Journal of Bone and Mineral Research* **5**:437-442.

Tawse-Smith, A., Payne, A.G., Kumara, R. & Thomson, W.M. (2002) Early loading of unsplinted implants supporting mandibular overdentures using a one-stage operative procedure with two different implant systems: a 2-year report. *Clinical Implant Dentistry and Related Research* **4**:33-42.

Taylor, K.F., Inoue, N., Rafiee, B., Tis, J.E., McHale, K.A. & Chao, E.Y. (2006) Effect of pulsed electromagnetic fields on maturation of regenerate bone in a rabbit limb lengthening model. *The Journal of Orthopaedic Research* **24**:2-10.

Wang, J., An, Y., Li, F., Li, D., Jing, D., Guo, T., Luo, E. & Ma, C. (2014) The effects of pulsed electromagnetic field on the functions of osteoblasts on implant surfaces with different topographies. *Acta biomaterialia* **10**: 975-985.

Wang, J., Tang, N., Xiao, Q., Zhang, L., Li, Y., Li, J., Zhao, Z. & Tan, L. (2015) Pulsed electromagnetic field may accelerate in vitro endochondral ossification. *Bioelectromagnetics* **36**: 35-44.

Yasuda, I. (1955) Dynamic callus and electric callus. *The Journal of Bone and Joint Surgery* **37A**:1292-1299.

Figure legends

Figure 1. Drawing of the device and inserted cap on the implants.

Figure 2. µCT analyses of control and test group performed after 2 and 4 weeks after surgery. It was performed separately into two subregions, where the region from the healing abutment to half the length of the implant was defined as "coronal" region, and the distant half as the "apical" region.

Figure 3. µCT morphometric analysis of the peri-implant trabecular bone in the coronal subregion. Scatter plots and Mean±SD for the control (blue) and test (red) groups. *p<0.05, test vs. control at the indicated time point; **p<0.05, test vs. control for the entire follow-up period; #p<0.05, time effect.

Figure 4. µCT morphometric analysis of the peri-implant trabecular bone in the full and apical subregions. Scatter plots and Mean±SD for the control (blue) and test (red) groups. *p<0.05, test vs. control at the indicated time point; **p<0.05, test vs. control for the entire follow-up period; #p<0.05, time effect.

Figure 5. Histological evaluation of the peri-implant bone. Two weeks post-surgery, in the control group, it was possible to observe the presence of newly formed bone in the coronal and apical portions; in the test group, 2 weeks post-surgery, bone trabeculae were found directly on the implant surface in the coronal, middle and apical portions of the implant. Four weeks post-surgery, in the control group bone trabeculae were found in the coronal and apical portions of the implant; in the test group lamellar and woven bone were observed in direct contact with the entire perimeter of the implant surface with no gaps at the bone-implant interface.

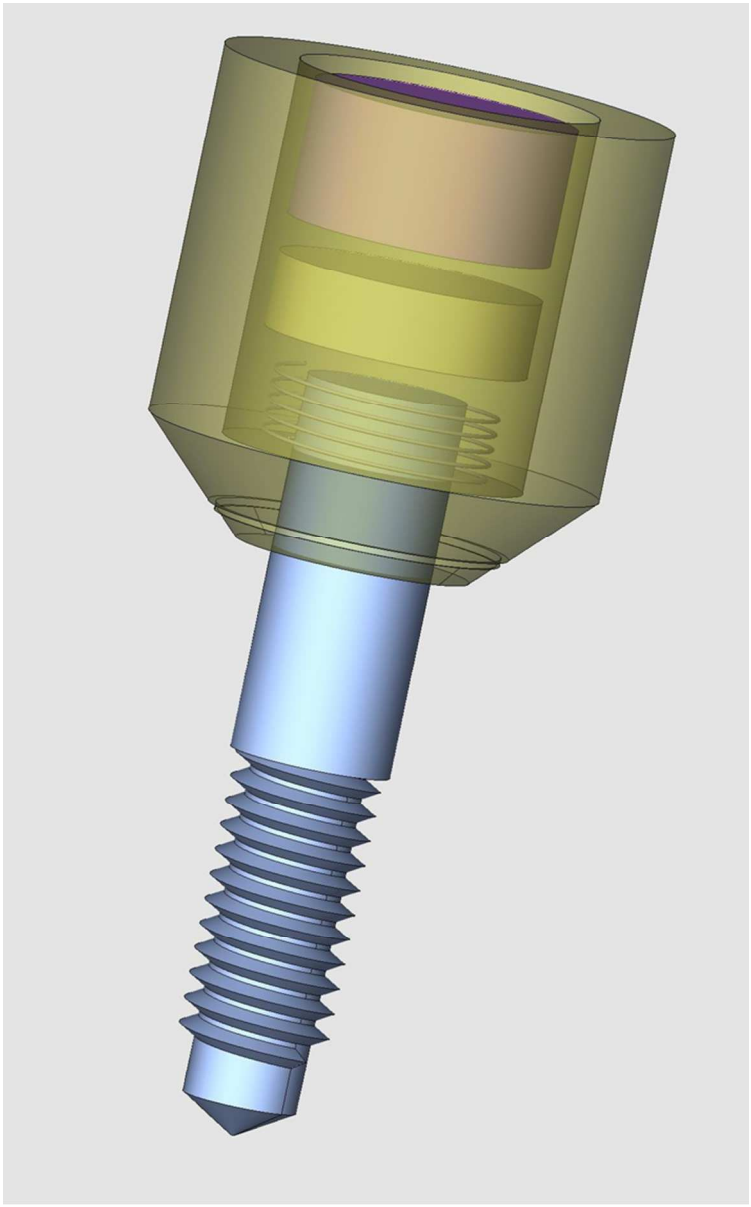

Drawing of the device and inserted cap on the implants.
60x96mm (300 x 300 DPI)

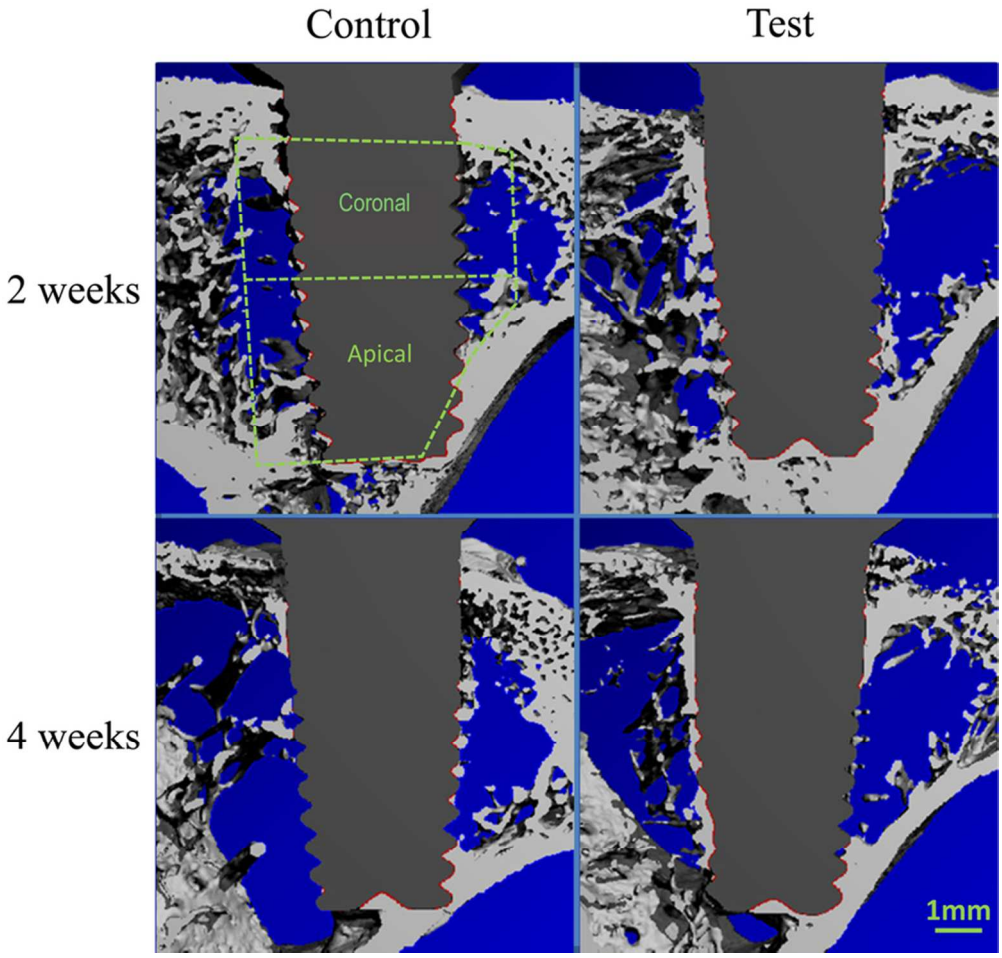

μCT analyses of control and test groups performed after 2 and 4 weeks after surgery. It was conducted separately into two subregions, where the region from the healing abutment to half the length of the implant was defined as "coronal" region, and the distant half as the "apical" region.
80x75mm (300 x 300 DPI)

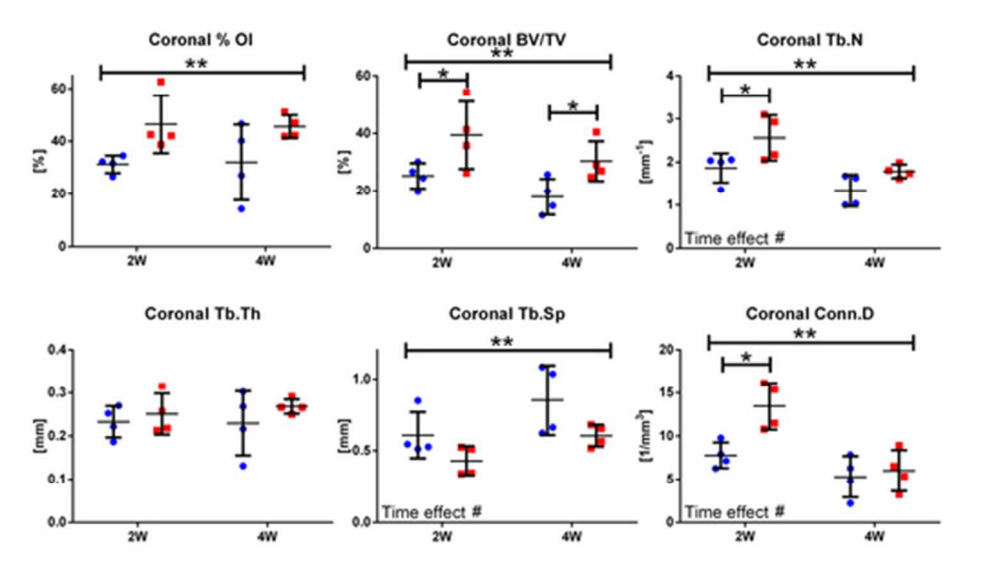

µCT morphometric analysis of the peri-implant trabecular bone in the coronal subregion. Scatter plots and Mean±SD for the control (blue) and test (red) groups. *p<0.05, test vs. control at the indicated time point; **p<0.05, test vs. control for the entire follow-up period; #p<0.05, time effect.
46x27mm (300 x 300 DPI)

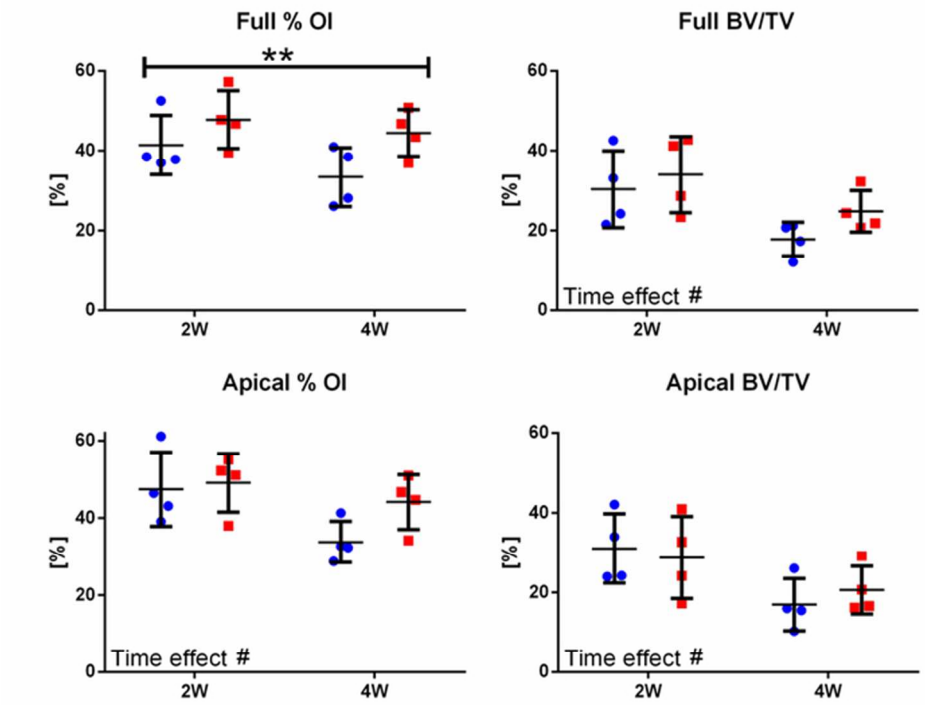

µCT morphometric analysis of the peri-implant trabecular bone in the full and apical subregions. Scatter plots and Mean±SD for the control (blue) and test (red) groups. *p<0.05, test vs. control at the indicated time point; **p<0.05, test vs. control for the entire follow-up period; #p<0.05, time effect.
63x49mm (300 x 300 DPI)

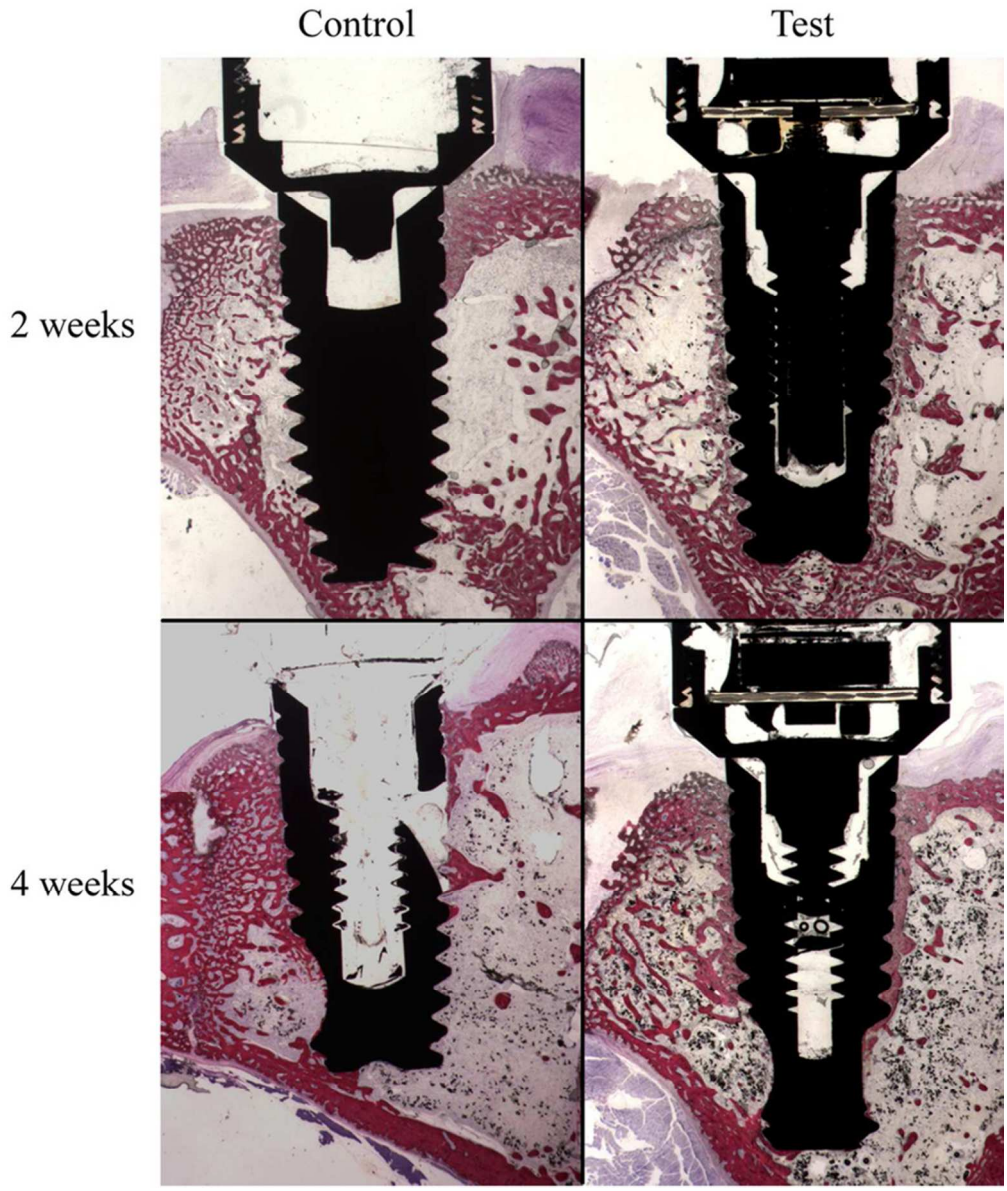

Histological evaluation of the peri-implant bone. Two weeks post-surgery, in the control group, it was possible to observe the presence of newly formed bone in the coronal and apical portions; in the test group, 2 weeks post-surgery, bone trabeculae were found directly on the implant surface in the coronal, middle and apical portions of the implant. Four weeks post-surgery, in the control group bone trabeculae were found in the coronal and apical portions of the implant; in the test group lamellar and woven bone were observed in direct contact with the entire perimeter of the implant surface with no gaps at the bone-implant interface (Toluidine blue and acid fuchsin 12x).
80x94mm (300 x 300 DPI)

Table 1. Morphometric parameters calculated using μCT in the PIB around control and test implants. Median, Mean±SD and % difference between groups are indicated for the coronal, apical and full regions, 2 and 4 weeks post implant insertion in 4 animals per group and time point.

		2W					2W and 4W
Parameter	Unit	Control/Test (Median)	Control (Mean±SD)	Test (Mean±SD)	% difference vs. control	Multiplicity adjusted p-value	Adjusted p-value
Coronal							
%OI	[%]	32.03/42.3	31.33±3.32	46.51±10.94	48.46	**0.0821 (ns)**	**0.0102 ****
BV/TV	[%]	25.58/38.49	25.24±4.35	39.39±11.39	56.03	**0.0484 ***	**0.0052 ****
Conn.D	[mm^{-3}]	7.53/13.44	7.78±1.49	13.46±2.70	73.11	**0.0086 ***	**0.0164 ****
Tb.N	[mm^{-1}]	2.02/2.55	1.87±0.34	2.56±0.53	37.42	**0.0411 ***	**0.0093 ****
Tb.Th	[mm]	0.24/0.24	0.23±0.04	0.25±0.05	7.69	**0.6105 (ns)**	**0.2664 (ns)**
Tb.Sp	[mm]	0.54/0.43	0.61±0.16	0.43±0.10	-29.16	**0.1398 (ns)**	**0.0204 ****
Apical							
%OI	[%]	44.76/51.63	47.43±9.62	49.10±7.58	3.52	**0.7622 (ns)**	**0.1382 (ns)**
BV/TV	[%]	29.16/28.48	31.10±8.65	28.77±10.67	-7.48	**0.7783 (ns)**	**0.8652 (ns)**
Full							
%OI	[%]	38.1/47.26	41.41±7.44	47.78±7.27	15.4	**0.2211 (ns)**	**0.0283 ****
BV/TV	[%]	28.66/34.67	30.35±9.56	33.98±9.53	12.0	**0.505 (ns)**	**0.1836 (ns)**

		4W				
Parameter	Unit	Control/Test (Median)	Control (Mean±SD)	Test (Mean±SD)	% difference vs. control	Multiplicity adjusted p-value
Coronal						
%OI	[%]	33.68/44.33	32.08±14.35	45.54±4.38	41.98	**0.0821 (ns)**
BV/TV	[%]	17.38/28.08	18.01±6.20	30.38±6.91	68.73	**0.0484 ***
Conn.D	[mm^{-3}]	5.56/5.92	5.29±2.40	5.99±2.39	13.23	**0.6733 (ns)**
Tb.N	[mm^{-1}]	1.34/1.78	1.34±0.37	1.79±0.16	33.52	**0.1124 (ns)**
Tb.Th	[mm]	0.24/0.27	0.23±0.07	0.27±0.02	16.78	**0.4851 (ns)**
Tb.Sp	[mm]	0.85/0.61	0.85±0.24	0.60±0.08	-28.94	**0.0945 (ns)**
Apical						
% OI	[%]	32.51/45.67	33.84±5.30	44.13±7.03	30.4	**0.1475 (ns)**
BV/TV	[%]	15.75/18.67	16.98±6.62	20.68±6.06	21.78	**0.7783 (ns)**
Full						
% OI	[%]	33.24/45.09	33.37±7.35	44.47±5.85	33.3	**0.0886 (ns)**
BV/TV	[%]	19.14/23.11	17.90±4.24	24.80±5.13	38.5	**0.3841 (ns)**

*$p<0.05$, test vs. control in the indicate time point

**$p<0.05$, test vs. control for the entire follow-up period (combined 2 and 4 weeks post-implantation).